NUMERICAL ANALYSIS OF THE FLOW BEHAVIOR PAST AN AHMED BODY WITH VARYING FRONT RADIUS CURVATURE AND ITS IMPLICATIONS IN THE AERODYNAMIC FORCES.

Raul Victor Teixeira Rosseto, Augusto Salomão Bornschlegell

Engineering Faculty, Federal University of Grande Dourados
Rodovia Dourados/Itahum, Km 12, Cidade Universitária,
Dourados/MS, Zip-Code: 364, CEP: 79.804-970
raul07_rosseto@hotmail.com, augustosalomao@ufgd.edu.br

Abstract. The objective of the present study is to evaluate the dynamics of the air flow past the well-known Ahmed body benchmark where its original geometry has been changed. The modification consists in changing only the front radius curvature; 4 additional curvatures were evaluated. These 5 different geometries were evaluated for 4 different flow velocities, so that the Reynolds Number ranged from $4.8\text{x}10^3$ to $4.8\text{x}10^4$. The simulations were performed in the transient regime. The initial condition of the transient model is the result of the equivalent steady state model. Regarding the numerical schemes, the second order upwind was employed for the discretization of the Navier-Stokes advective terms, PISO algorithm for the pressure-velocity coupling and second order backward integration for the transient term. The k-omega SST standard OpenFOAM implementation was used as turbulence model. The local flow behavior at the frontal part of the Ahmed body, like boundary layer detachment and reattachment, as well as the its global physical behavior are exploited and correlated to the changes in the aerodynamic forces.

Keywords: Ahmed Body, OpenFOAM, Computational fluid dynamics, Numerical analysis

1 Introduction

A numerical analysis in fluid flow is one of the most effective and important tools in cases studies in fluid dynamics, because the numerical analysis gives us detailed information about the fluid flow and thus leads to a better understanding of the complex fluid flow. The improvement in the numerical methods used to solve the Navier-Stokes equations and the increase of the available computational processing in the recent decades has made possible, accordingly, the numerical evaluation of more complex flows. The study object of the present work is the well-known Ahmed body, Ahmed et al. [1], a simplified geometry of a passenger vehicle, which seeks to highlight important characteristics for aerodynamic studies, such as variation of external chamfer angle. This benchmark has been used for several studies since its publication by Syed R. Ahmed in 1984.

In Fig. 1, we have the original model, developed by Ahmed et al. [1]. Its geometry has several aspects, in which we can investigate the behavior of the drag and lift coefficient, detachment of the boundary layer, detachment of vortex and recirculation zones.

A large amount of the energy used in ground transportation is used to overcome aerodynamic drag, with typically over 60% of the total resistive force being aerodynamic drag at highway speeds Hucho [2]. Ahmed et al. [1] defined a similar body based on the fast-back shape of automobiles that has been accepted as the standard for aerodynamic studies on ground vehicles. Due to the wide variability in the shape of ground vehicles, on Aerodynamic Drag Mechanisms of Bluff Bodies et al. [3] defined a generalized three-dimensional model that produces a wake with features similar to the important ones in automobile wakes

It is well known in bluff-body aerodynamics that an increase in aspect ratio of a body tends to reduce three-

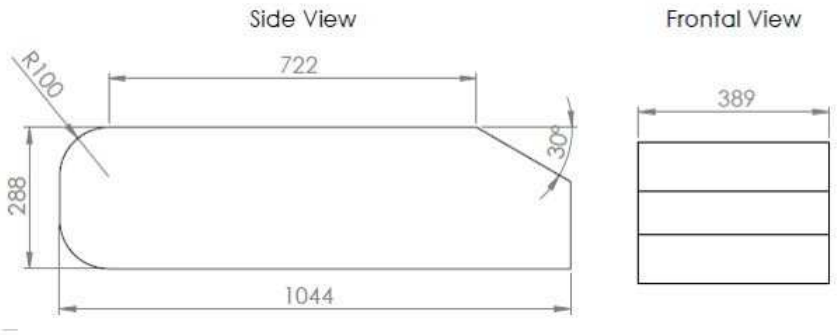

Figure 1. Ahmed Body (dimensions in millimeters)

dimensional effects by increasing the distance between the edge-affected flows. Huang and Hui [4] studied numerically the effect of aspect ratio on rectangular plates, finding that at low aspect ratio, the edge vortices stabilize the wake and increase the stall angle.

Many other studies have been performed to investigate the flow topologies around the Ahmed model. Since the low-pressure regions of the body are responsible for a large proportion of pressure drag, most of the studies focused on the wake structure behind the geometry. Bayraktar et al. [5] studied the influence of Reynolds number on the drag and lift coefficients of the Ahmed body. It was concluded by increasing the Reynolds number from $2.2\text{x}10^6$ to $13.2\text{x}10^6$, drag coefficient increases while lift coefficient is nearly constant.

Minguez et al. [6] and Rajsinh and Raj [7] performed experimental and numerical studies on the external flow and turbulent wake structures around the Ahmed body. Minguez et al. [6] used spectral vanishing viscosity LES (SVV-LES) method. His formulation needed no additional computational cost of the SVV-LES with respect to DNS. Rajsinh and Raj [7] used Spalart-Allmaras turbulence model and concluded this turbulent model could not predict the flow over the slant well at high Reynolds numbers.

Since the fuel consumption has become more important over the last few decades, many studies were performed on the reduction of the drag coefficient. For example, Khaled et al. [8] studied a simplified car model with air inlets and outlets including a real cooling system and a simplified engine block. Their configurations could decrease drag and lift coefficient by 2% and 5% and aerodynamic cooling coefficient by 50% respectively. [9] employed some instruments like a rear screen, rear fairings, and vortex generators that resulted in the drag reduction up to 6.5%, 26% and 1.24%, respectively. [10] showed that changing the slant angle of an Ahmed body from 30° to 20° could decrease the drag up to 8% and a 1.5 to 5% save on fuel consumption.

The lift and drag of this model are strongly influenced by the flow field around its edges. The upper and lower frontal curvature (R100 in Fig. 1) produce a transient and detached flow that induces resistance forces on the body. Changing this geometrical feature may affect different flow features which can significantly affect dynamic stability and comfort. The modeling studied in this work has the purpose of a comparative analysis between 5 frontal radius values for 4 different inlet velocities so that the Reynolds Numbers ranged from $4.8\text{x}10^3$ to $4.8\text{x}10^4$.

2 Numerical Model

The geometrical model to be studied is shown in Fig. 2. The image shows 5 different superimposed bodies showing the difference in the frontal radius without changing the other standard parameters. The first case called benchmark (5 mm radius for a scale of 1:20), is the standard radius of the original body developed by Ahmed et al. [1]. The geometry modification was applied to the radius in the x direction, maintaining the radius in the y direction, so that an ellipsoidal frontal geometry was evaluated.

For each geometry and each inlet velocity, two cases were evaluated, one in steady state regime and other in the transient regime. The permanent regime data (simpleFoam) were used as initial condition for the transient regime (pisoFoam), the final solver used for the analysis of the models. Both models are two-dimensional, due to the computer system with limited configurations to run the simulations, considering on the left of the computational domain, the inlet, on the right, the outlet, at the top, the slip boundary condition and, at the bottom, a moving wall boundary condition that represents the relative motion between the ground and the vehicle as shown in Fig. 3. In this figure, as well as in all the results images, the axis are in meters.

The intermediate mesh, created with a tridimensional mesher tool (snappyHexMesh) was composed of 3754581

Figure 2. Differences of the studied models

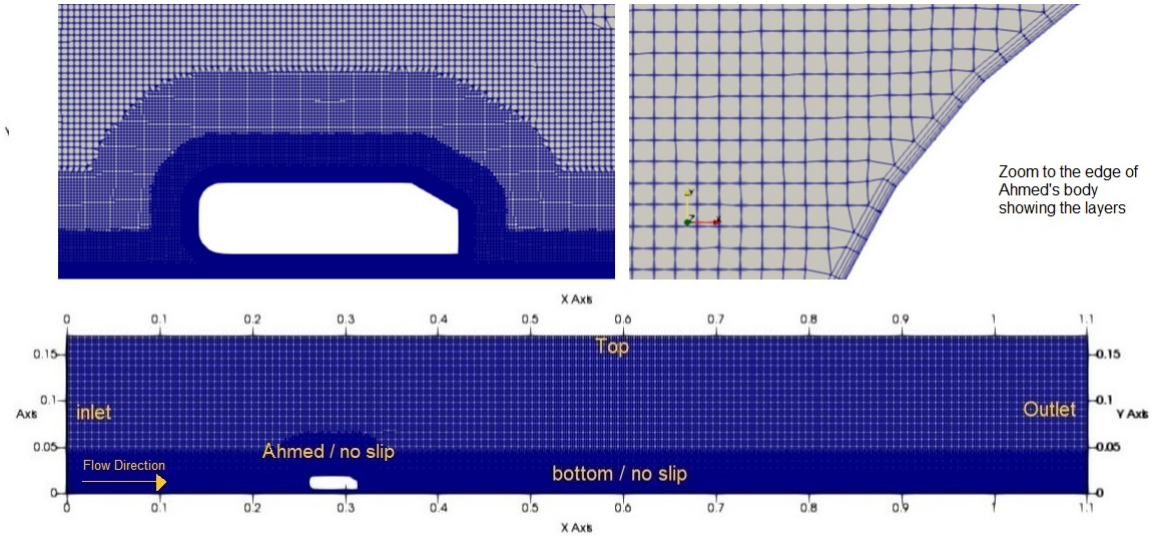

Figure 3. Mesh and boundary conditions, axis in meters

cells. In order to create a 2D mesh, the frontal patch was extruded in 5 mm, so that the final mesh configuration had 338824 cells. The mesh sensibility analysis demonstrates difference below 2.4% in the aerodynamic forces when compared with a finer mesh (684489 cells). Mesh layers were added to the Ahmed body surface in order to create a refinement that guarantees a yPlus less than 1. Regarding the numerical schemes, the second order upwind was employed for the discretization of the Navier-Stokes advective terms, PISO algorithm for the pressure-velocity coupling and second order backward integration for the transient term. The standard OpenFOAM K-omega SST turbulence model Menter et al. [11] was used with a turbulent intensity of 3%. Both turbulence model and intensity were arbitrated according to the employed mesh and the available computational processing. The total physical time for the simulation is 2 seconds. Four velocities were defined and 4 Reynolds numbers were evaluated, with velocities of 5, 10, 20 and 50 m/s for Re = $4.8\text{x}10^3$; $9.6\text{x}10^3$; $1.92\text{x}10^4$; $4.8\text{x}10^4$ respectively. To control the timestep, the Courant number was set in 1 and the variable time step was used. The Reynolds number is defined by equation (1):

$$Re = \frac{\rho U L}{\mu} \tag{1}$$

where ρ stands for the air density [kg.m^{-3}], V represents the free stream velocity [m.s^{-1}], L represents the Ahmed's body height [m] and μ stands for the air viscosity [Pa.s]. The pisoFoam solver, to solve the continuity equation and the moment equation respectively:

$$\nabla \cdot V = 0 \tag{2}$$

$$\rho \frac{DV}{Dt} = -\nabla P + \rho g + \mu \nabla^2 V \tag{3}$$

For the Eq. (2) we have the divergence of velocity and for the Eq. (3) we have the material derivative of velocity, ∇P represents the pressure gradient, ρg are the gravitational field forces and $\mu \nabla^2 V$ is the Laplacian of velocity.

3 Results and Discussion

The drag coefficient obtained for the benchmark models are in agreement with the available literature data (Bruneau et al. [12], Korkischko [13], Ahmed et al. [1]) for the corresponding Re range, as illustrated in Fig. 4. For Re = 15000 compared to the literature models of Ahmed et al. [1] and Korkischko [13] it was validated for a difference of only 4.33%. For Re = 30000, when compared to the Bruneau et al. [12], the difference in the drag coefficient is 44.82%.

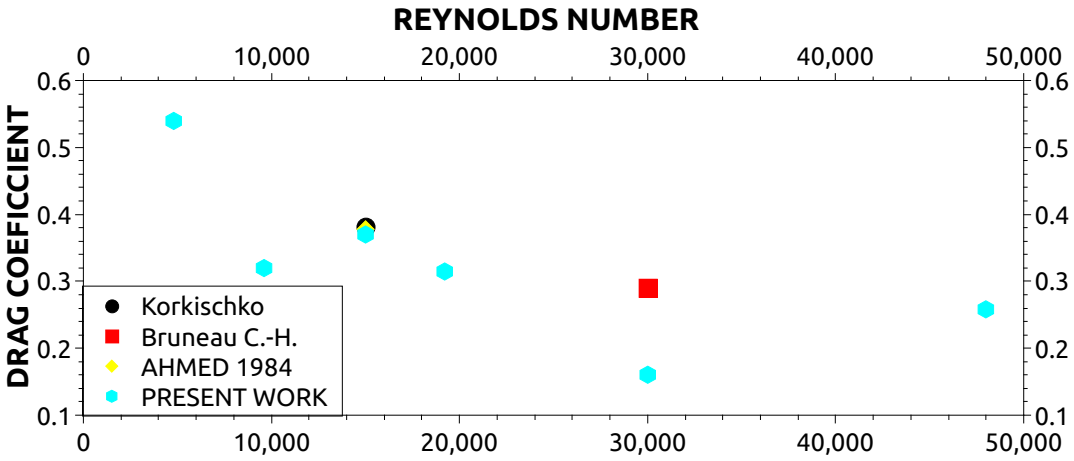

Figure 4. Validation of results

The velocity and pressure fields and the variation of the drag coefficient are presented for five cases with 4 different velocities, totaling 20 cases. Considering a simulation time from 0 to 2 seconds and considering a width of 0.01 m in order to maintain the Ahmed pattern, the drag coefficients for each case are represented in Fig. 5, where the benchmark is the original Ahmed body. For better evaluations of the drag coefficient, the results after the instant t = 1s were considered, where there is a stabilization in the coefficients. This was not the case for the benchmark at U = 5 m/s, where stabilization is reached from 1.7 s on.

Evaluating the behavior of drag coefficients over time, for Reynolds of $4.8 \text{x} 10^3$, there is a numerical instability at the beginning of the resolution in transient regime up to 0.5 s. From this moment on, the simulation stabilizes with the drag coefficient around 0.32, demonstrating that changing the radius for this Reynolds number does not cause any change in the drag coefficient. For the Benchmark, it is observed in Fig. 6 the displacement of the boundary layer right after the frontal curvature, which promotes a wider wake, and a greater pressure difference between the front and rear of the Benchmark. With an increase in this curvature, the boundary layer detachment is no longer present and, the drag coefficient remains constant. In Fig. 7 that for the probes from x = 0.27 to 0.31 m demonstrate negative velocity values, evidencing recirculation bubbles in the flow at the rear of Ahmed's body.

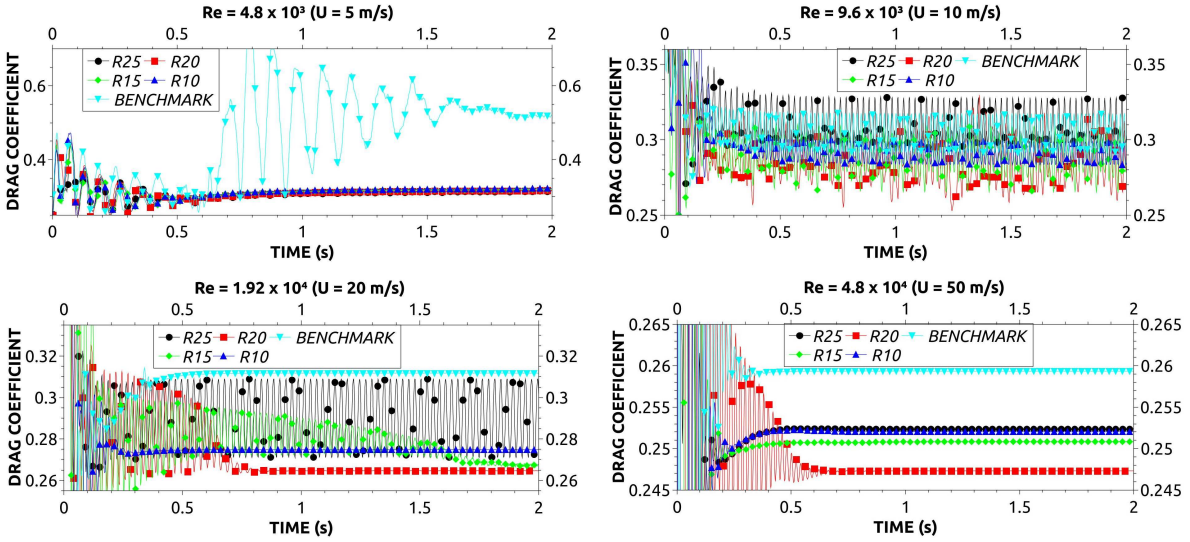

Figure 5. Variations of drag coefficient for different Re

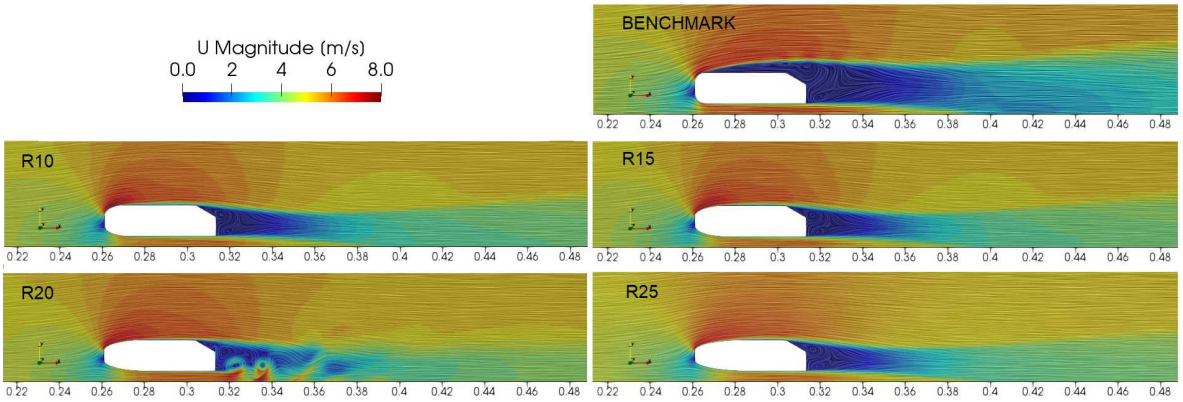

Figure 6. U = 5 m/s velocity for different geometries, x axis in meters

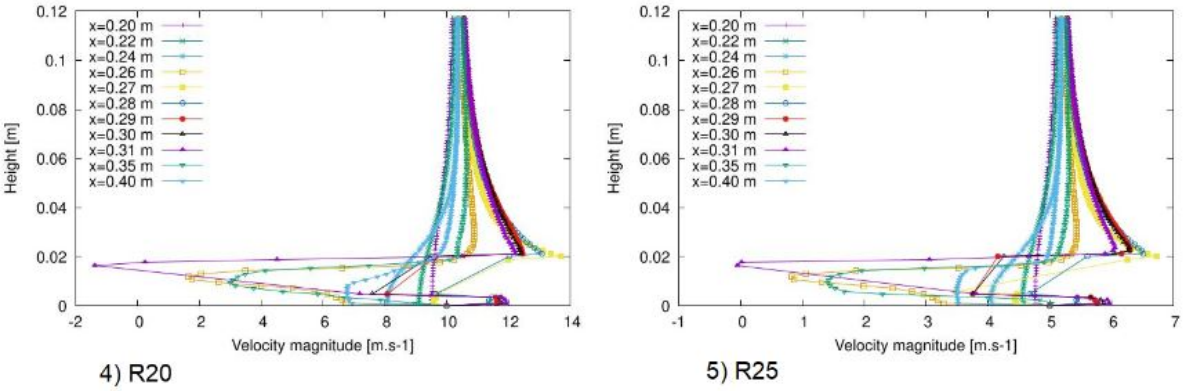

Figure 7. U = 5 m/s velocity for different radius along the distance.

For the analysis of Re 9.6x10^3, the drag coefficient for all radius oscillates around 0.3, this oscillation happens from the wake interaction with the ground. As the oscillation remains for the entire simulation, there are a calculated frequencies of 39.8 to 65.4 Hz for the geometries and a average Strouhal Number of 0.00549. The corresponding flow field is presented in Fig. 8.

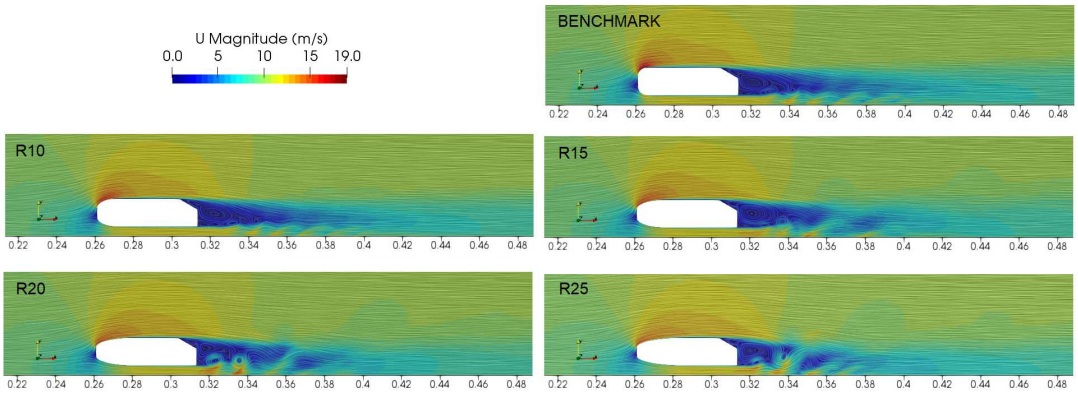

Figure 8. U = 10 m/s velocity for different geometries, x axis in meters

The periodicity that was previously observed for Re = 9.6x10^3 does not exist in this case for radius smaller than 20 mm, keeping the periodicity only for the radius of 25 mm. In Fig. 9 it is noted for R25 turbulent structures, which are detached from the Ahmed body, generating shedding vortex which cases the periodic behavior, at a calculated frequency of 43.48 Hz and Strouhal Number = 0.002174. As the radius increases it promotes the passage of fluid in the lower part of Ahmed's body, making the speed magnitudes of the R25 greater than the others.

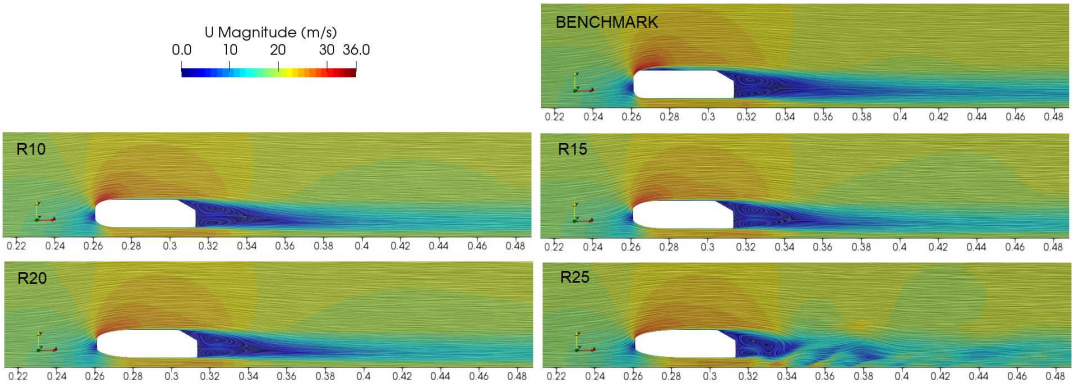

Figure 9. U = 20 m/s velocity for different geometries, x axis in meters

For 4.8x10^4 Reynolds, the periodic behavior is extinct, and it is observed that, in relation to the Benchmark, with the increase of the radius, the drag coefficient decreases, with the exception of R25 which presents a drag coefficient greater than the underlying radius R10, R15 and R25. It is worth to mention that for this Re, all the drag coefficients are between 0.245 and 0.26, so that the drag coefficient nearly do not change with the radius curvature. The corresponding flow fields are presented in Fig. 10.

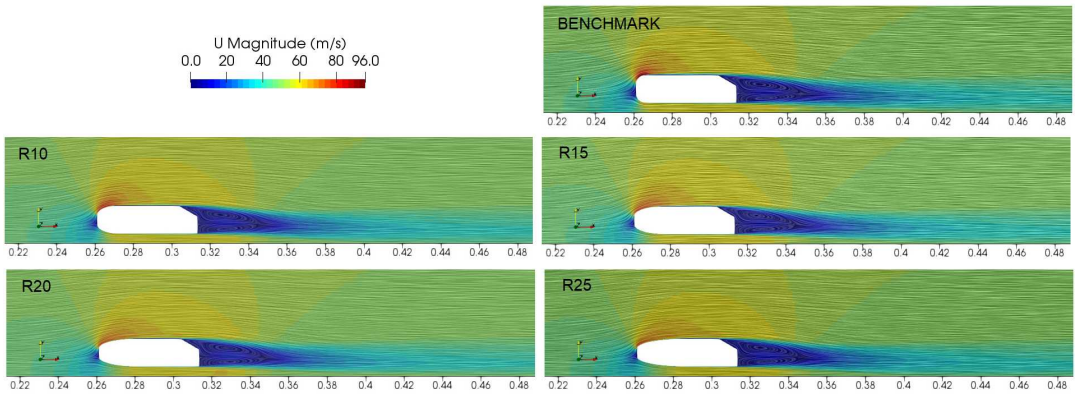

Figure 10. U = 50 m/s velocity for different geometries, x axis in meters

4 Conclusions

For the different frontal curvatures studied, it was observed that for the Re of $4.8\text{x}10^3$, the flow behavior is quasi-static. As Re increases to $9.6\text{x}10^3$, it starts to have a periodic behavior flow, which is maintained only for R25 when we increase the Reynolds number. This oscillatory behavior is completely extinguished for Re of $4.8\text{x}10^4$. It is also noted that the best results for the lowest drag coefficients for all cases, is found in R20.

References

[1] S. R. Ahmed, G. Ramm, and G. Faltin. Some salient features of the time -averaged ground vehicle wake. *SAE International*, vol. 93, n. 2, pp. 473–503, 1984.
[2] W.-H. Hucho. Aerodynamics of road vehicles. *Annu. Rev. Fluid Mech.*, 1993.
[3] on Aerodynamic Drag Mechanisms of S. Bluff Bodies, R. Vehicles, G. Sovran, W. T. Mason, T. Morel, and G. M. Corporation. *Aerodynamic drag mechanisms of bluff bodies and road vehicles / edited by Gino Sovran, Thomas Morel, and William T. Mason, Jr.* Plenum Press New York, 1978.
[4] H. Huang and D. Hui. Large-amplitude vibration of imperfect angle-ply laminated rectangular plates for various materials. *World Journal of Engineering*, vol. 12, n. 4, pp. 313–318, 2015.
[5] I. Bayraktar, D. Landman, and O. Baysal. Experimental and computational investigation of ahmed body for ground vehicle aerodynamics. *SAE Technical Paper 2001-01-2742*, 2001.
[6] M. Minguez, R. Pasquetti, and E. Serre. Spectral vanishing viscosity stabilized les of the ahmed body turbulent wake. *Communication in Computational Physics*, pp. 635–648, 2009.
[7] C. Rajsinh and R. T. K. Raj. Numerical investigation of external flow around the ahmed reference body using computational fluid dynamics. *Research Journal of Recent Science*, pp. 1–5, 2012.
[8] M. Khaled, H. Elhage, F. Harambat, and H. Peerhossaini. Some innovative concepts for car drag reduction: A parametric analysis of aerodynamic forces on a simplified body. *Journal of Wind Engineering and Industrial Aerodynamics*, pp. 36–47, 2012.
[9] U. S. Rohatgi. Methods of reducing vehicle aerodynamic drag. *ASME 2012 Summer Heat Transfer Conference Puerto Rico*, 2012.
[10] P. R. Sonawane, S. P. Sekhawat, and K. Rajput. Aerodynamic analysis of car body for minimum fuel consumption. *Journal of Information Knowledge and Research, Mechanical Engineering*, pp. 54–57, 2011.
[11] F. R. Menter, M. Kuntz, and R. Langtry. Ten years of industrial experience with the sst turbulence model. *In Pro-ceedings of the fourth international symposium on turbulence, heat and mass transfer*, vol. 4, n. 1, pp. 625–638, 2003.
[12] C.-H. Bruneau, I. Mortazavi, and P. Gilliéron. Passive control around the two-dimensional square back ahmed body using porous devices. *J. Fluids Eng.*, vol. 130, pp. 1–33, 2008.
[13] I. Korkischko. *Experimental investigation and numerical simulation of the flow around an automobile model: Ahmed's body (in Portuguese)*. PhD thesis, Graduate Program in Mechanical Engineering, Polytechnic School of the University of São Paulo, São Paulo, Brasil, 2006.